Supporting Information

Probing the Electronic Structure and Spectroscopy of the Pyrrolyl and Imidazolyl Radicals using High-Resolution Photoelectron Imaging of Cryogenically-Cooled Anions

Yue-Rou Zhang‡ , Dao-Fu Yuan‡ , and Lai-Sheng Wang

Department of Chemistry, Brown University, Providence, Rhode Island 02912, USA. E-mail: Lai-Sheng_Wang@brown.edu

‡ Equal contribution.

Table of Contents

1 Experimental Procedures

1.1 Experimental methods

The experiment was carried out using our third-generation ESI-PES apparatus.[1] The pyrrole and imidazole samples were purchased from Sigma-Aldrich with a specified purity (98% for pyrrole and 99% for imidazole) and used without further purification. The pyrrolide or imidazolide anions were produced by electrospray of a 1 mM solution of pyrrole or imidazole in a mixed solvent of CH_3OH/H_2O (9:1 volume ratio) at pH~10. Anions generated in the ESI source[2] were guided by a set of quadrupole and octupole ion guides into a cryogenically-cooled 3D Paul trap operated at 4.6 K.[3] After being accumulated for about 0.1 s and thermally cooled via collisions with 1 mTorr He/H_2 (4/1 volume) background gas, the anions were pulsed out of the trap at a repetition rate of 10 Hz, and entered the extraction zone of a time-of-flight mass spectrometer. The pyrrolide and imidazolide anions were selected by a mass gate and then photodetached in the interaction zone of a velocity-map imaging lens[4] by a Nd:YAG laser or a tunable dye laser. The propagation and polarization directions of the detachment laser were parallel to the imaging plane. Photoelectrons were projected onto a pair of 75-mm diameter micro-channel plates coupled to a phosphor screen and captured by a charge-coupled-device camera. The PE images were inverted using pBASEX[5] and BASEX.[6] The PE spectra were calibrated with the known spectra of Au^- at different photon energies. The kinetic energy (KE) resolution was 3.8 cm^{-1} for electrons with 55 cm^{-1} KE and 1.5% ($\Delta KE/KE$) for KE above 1 eV in the current experiment.

1.2 Calculation methods

Geometry optimization and ground-state electronic structure calculations were performed using density functional theory (DFT) at the B3LYP/6-311++(d,p) level of theory. The electronic structure calculations were followed by vibrational analyses. All electronic structure calculations were preformed using Gaussian 09.[7] Franck-Condon factor calculations were carried out using the FC-Lab2 program.[8]
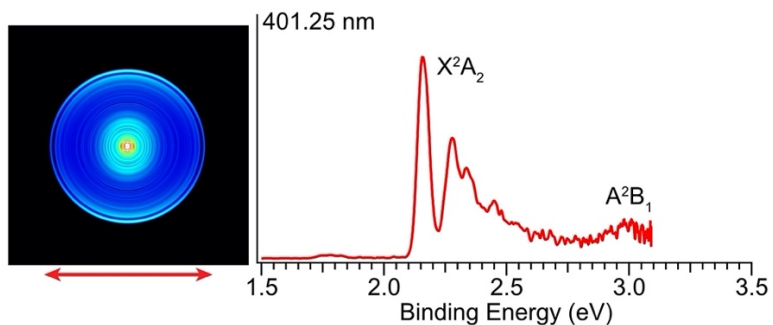
2 Supplementary Figures

Fig. S1 Photoelectron image and spectrum of the pyrrolide anion at 401.25 nm (3.0900 eV). The weak feature around 1.75 eV is due to the presence of a small amount of the 2-pyrrolide isomer. The double arrow indicates the polarization direction of the detachment laser.
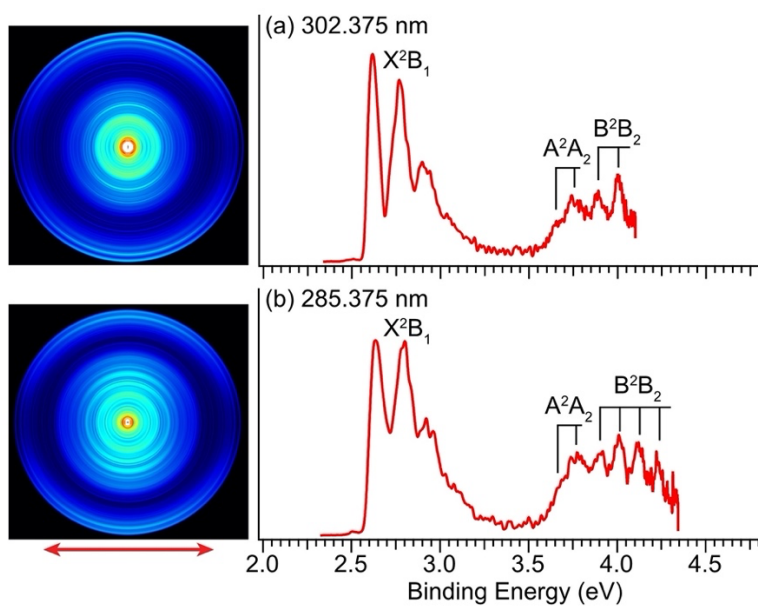

Fig. S2 Photoelectron images and spectra of the imidazolide anion at (a) 302.375 nm (4.1003 eV) and (b) 285.375 nm (4.3446 eV). The double arrow indicates the polarization direction of the detachment laser.
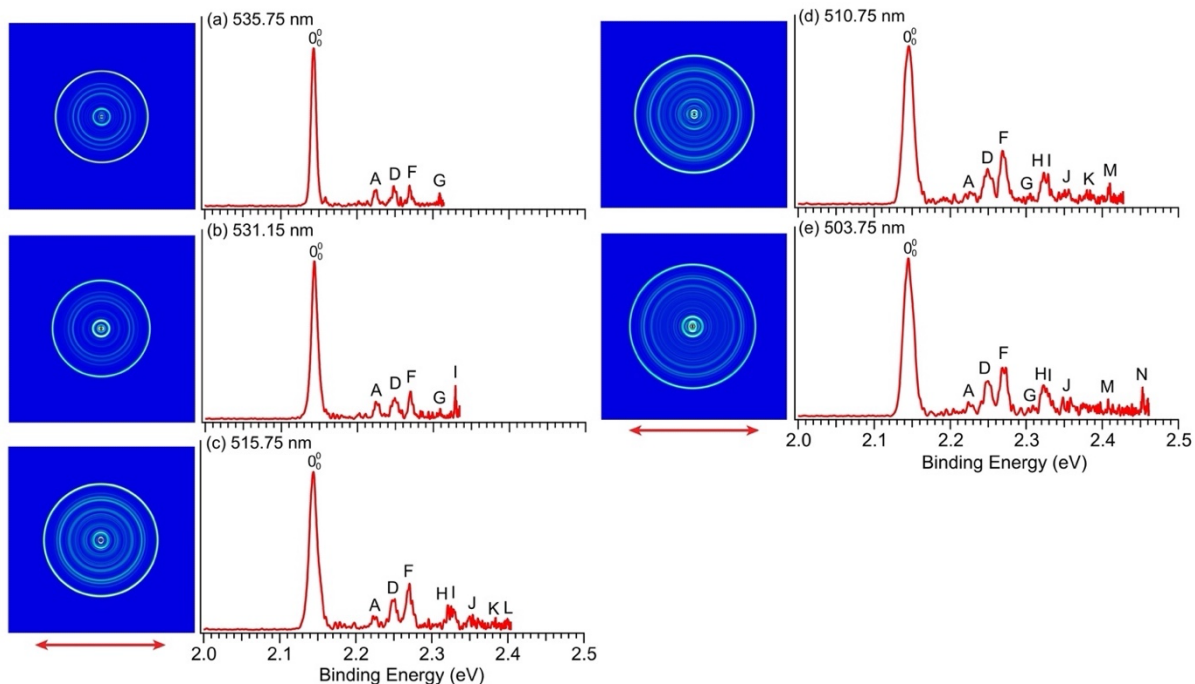
Fig. **S3** Photoelectron images and spectra of the pyrrolide anion at (a) 535.75 nm (2.3142 eV), (b) 531.15 nm (2.3343 eV), (c) 515.75 nm (2.4040 eV), (d) 510.75 nm (2.4275 eV) and (e) 503.75 nm (2.4612 eV). The double arrows indicate the polarization direction of the detachment laser.

Fig. **S4** Photoelectron images and spectra of the imidazolide anion at (a) 451.95 nm (2.7433 eV), (b) 450.75 nm (2.7506 eV), (c) 439.75 nm (2.8194 eV), (d) 437.95 nm (2.8310 eV) and (e) 427.75 nm (2.8985 eV). The double arrows indicate the polarization direction of the detachment laser.

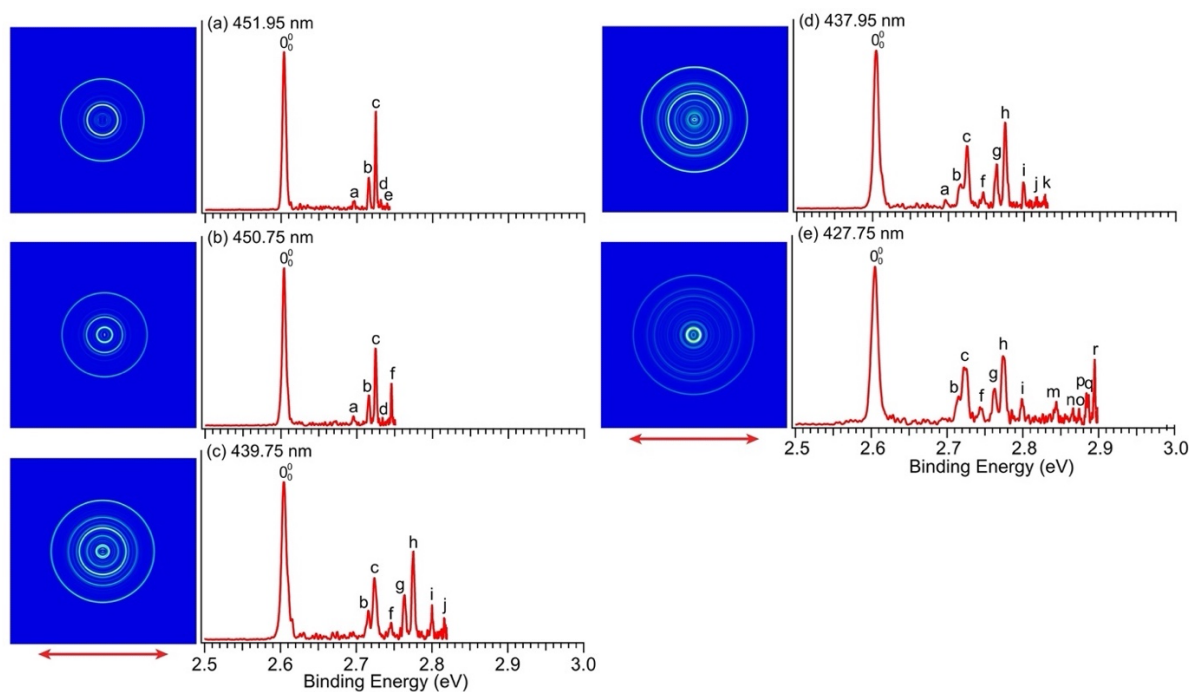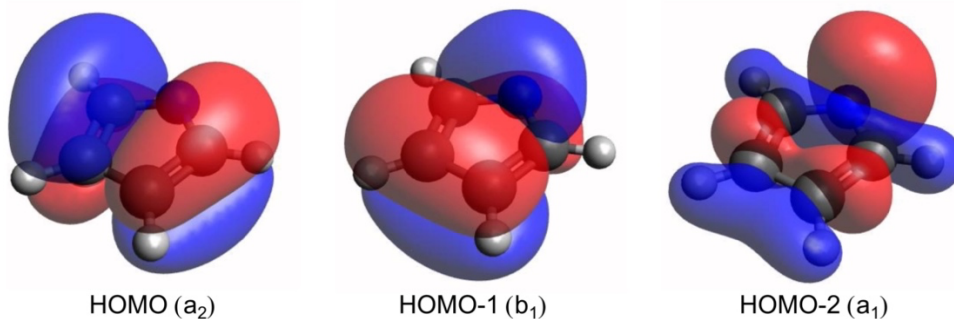**Fig**. **S5** The valence molecular orbitals of the pyrrolide anion (isovalue = 0.02).

HOMO (a_2)　　HOMO-1 (b_1)　　HOMO-2 (a_1)

HOMO (b_1)　　HOMO-1 (a_2)　　HOMO-2 (b_2)
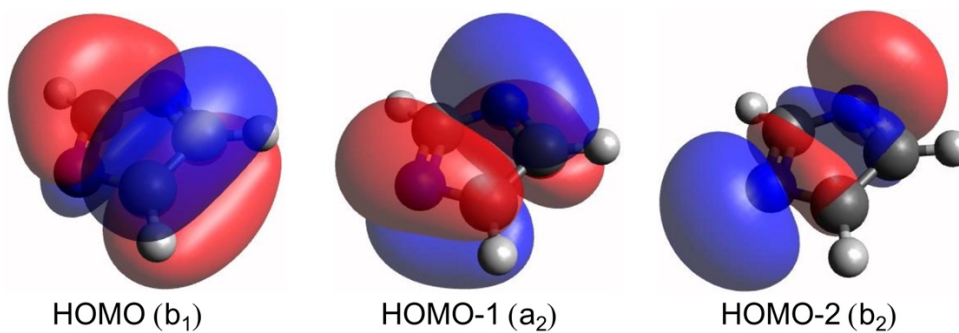
Fig. S6 The valence molecular orbitals of the imidazolide anion (isovalue = 0.02).

v_1 = 3246 cm^{-1}　v_2 = 3201 cm^{-1}　v_3 = 1556 cm^{-1}　v_4 = 1433 cm^{-1}　v_5 = 1202 cm^{-1}　v_6 = 1090 cm^{-1}　v_7 = 1043 cm^{-1}

v_8 = 882 cm^{-1}　v_9 = 904 cm^{-1}　v_{10} = 817 cm^{-1}　v_{11} = 488 cm^{-1}　v_{12} = 835 cm^{-1}　v_{13} = 710 cm^{-1}　v_{14} = 540 cm^{-1}

v_{15} = 3227 cm^{-1}　v_{16} = 3197 cm^{-1}　v_{17} = 1355 cm^{-1}　v_{18} = 1293 cm^{-1}　v_{19} = 1079 cm^{-1}　v_{20} = 935 cm^{-1}　v_{21} = 664 cm^{-1}

Fig. **S7** The atomic displacement vectors of the vibrational modes for pyrrolyl. The frequencies are shown below for each mode.
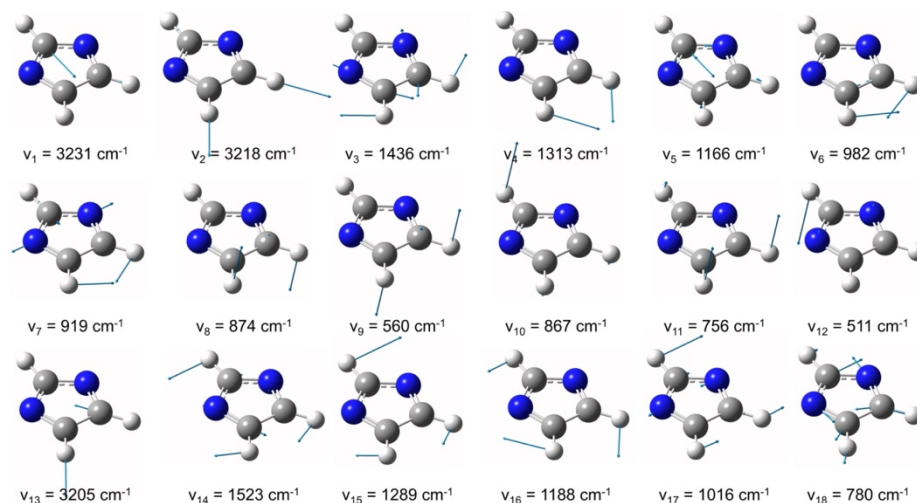
Fig. S8 The atomic displacement vectors of the vibrational modes for imidazolyl. The frequencies are shown below for each mode.

v_1 = 3231 cm^{-1} v_2 = 3218 cm^{-1} v_3 = 1436 cm^{-1} v_4 = 1313 cm^{-1} v_5 = 1166 cm^{-1} v_6 = 982 cm^{-1}

v_7 = 919 cm^{-1} v_8 = 874 cm^{-1} v_9 = 560 cm^{-1} v_{10} = 867 cm^{-1} v_{11} = 756 cm^{-1} v_{12} = 511 cm^{-1}

v_{13} = 3205 cm^{-1} v_{14} = 1523 cm^{-1} v_{15} = 1289 cm^{-1} v_{16} = 1188 cm^{-1} v_{17} = 1016 cm^{-1} v_{18} = 780 cm^{-1}
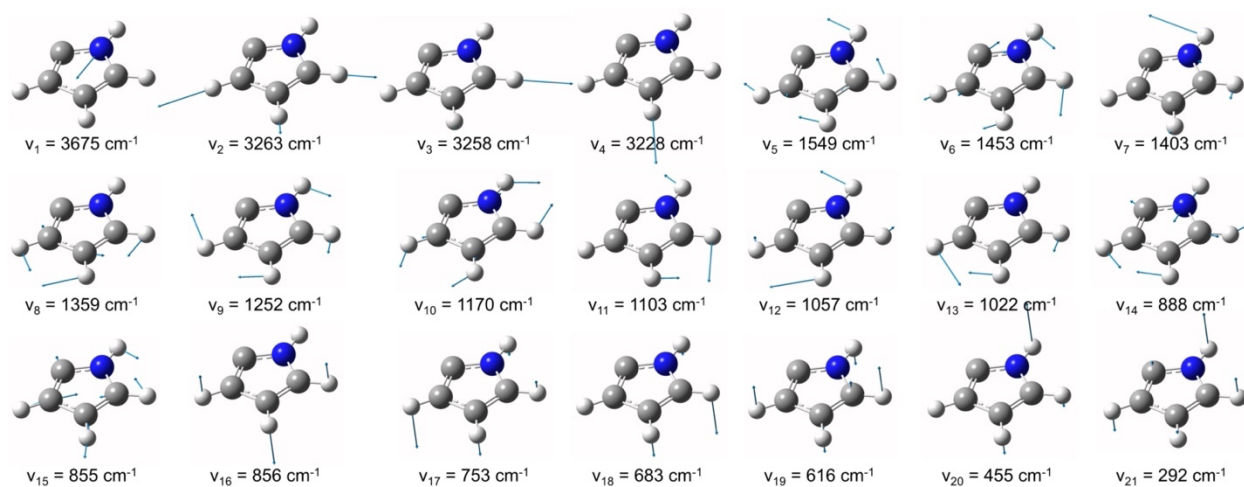
Fig. S9 The atomic displacement vectors of the vibrational modes for 2-pyrrolyl. The frequencies are shown below for each mode.
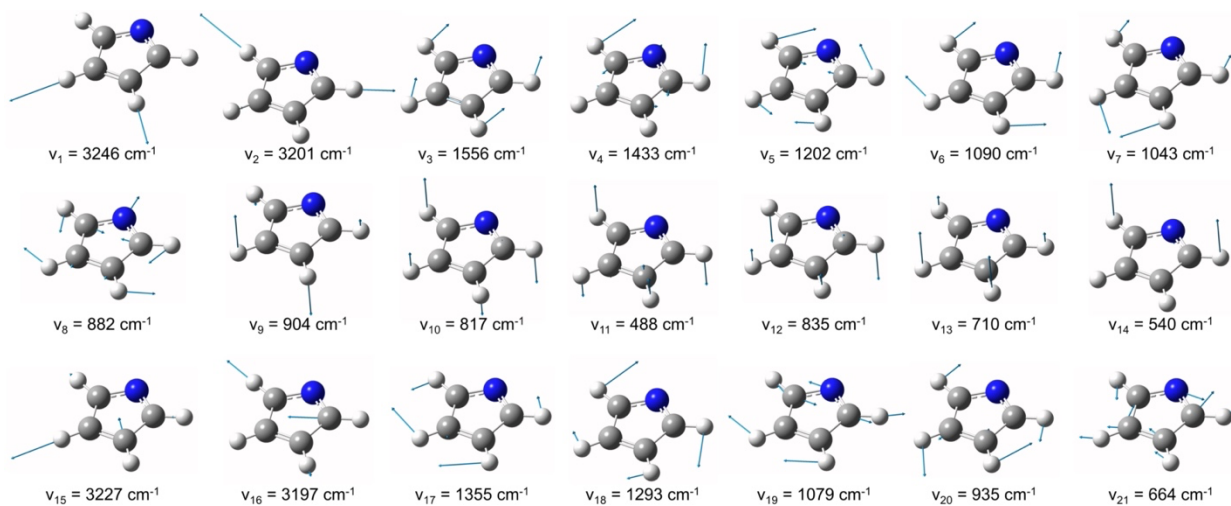
v_1 = 3675 cm^{-1} v_2 = 3263 cm^{-1} v_3 = 3258 cm^{-1} v_4 = 3228 cm^{-1} v_5 = 1549 cm^{-1} v_6 = 1453 cm^{-1} v_7 = 1403 cm^{-1}

v_8 = 1359 cm^{-1} v_9 = 1252 cm^{-1} v_{10} = 1170 cm^{-1} v_{11} = 1103 cm^{-1} v_{12} = 1057 cm^{-1} v_{13} = 1022 cm^{-1} v_{14} = 888 cm^{-1}

v_{15} = 855 cm^{-1} v_{16} = 856 cm^{-1} v_{17} = 753 cm^{-1} v_{18} = 683 cm^{-1} v_{19} = 616 cm^{-1} v_{20} = 455 cm^{-1} v_{21} = 292 cm^{-1}

3 Supplementary Tables

Table S1. The observed features for the 2-pyrrolide anion, with their binding energies (BEs), shifts relative to the 0–0 transition, asymmetry parameters (β), and assignments, compared with theoretical frequencies (ω).

Observed peak	BE (eV)[a]	BE (cm^{-1})[a]	Shift (cm^{-1})	β	Assignment	ω (cm^{-1})[b]	ω (cm^{-1})[c]
$^X0_0^{0'}$	1.6990(30)	13703(24)	0	-0.2	0-0 of ground state		
$^A0_0^{0'}$	1.7170(53)	13849(43)	146	0.1	0-0 of first excited state		
$^X1'$	1.7321(44)	13970(35)	267	-0.4	21^1	292	325.8
$^X2'$	1.7542(53)	14149(43)	446	-0.5	20^1	455	499.3
$^X3'$	1.7656(60)	14241(48)	538		21^2	584	651.6
$^X4'$	1.7824(33)	14376(27)	673	-0.5	18^1	683	695.7
$^X5'$	1.8034(54)	14545(44)	842	-0.4	$15^1/16^1$	855/856	846.0/842.0
$^X6'$	1.8319(36)	14775(29)	1072	-0.4	12^1	1057	1060.2

[a]The numbers in the parentheses indicate the experimental uncertainties in the last digit.

[b]The frequencies are calculated at the B3LYP/6-311++G** level of theory (see Figure S9 and Table S6).

[c]From reference 9, calculated at the fc-CCSD(T)/ANO level of theory.

Table S2. The observed vibrational modes and their frequencies for pyrrolyl from the current work, in comparison with the calculated values.

vibrational mode	symmetry	ω (exp) (cm^{-1})[a]	ω (theo) (cm^{-1})[b]	ω (theo) (cm^{-1})[c]
ν_{21}	b_2	656 (7)	664	668.3
ν_{13}	b_1	688 (7)	710	700.9
ν_{10}	a_2	808 (12)	817	815.0
ν_9	a_2	890 (8)	904	885.3
ν_8	a_1	844 (8)	882	869.5
ν_7	a_1	1018 (11)	1043	1039.1
ν_5	a_1	1224 (12)	1202	1188.6
ν_4	a_1	1446 (10)	1433	1447.3

[a]The numbers in the parentheses indicate the experimental uncertainties in the last digit.
[b]The theoretical frequencies are calculated at the B3LYP/6-311++G** level of theory. See Table S4.

[c]From ref. 9, calculated at the fc-CCSD(T)/ANO level of theory.

Table S3. The observed vibrational modes and their frequencies for imidazolyl from the current work, in comparison with the calculated values.

vibrational mode	symmetry	ω (exp) (cm^{-1})[a]	ω (theo) (cm^{-1})[b]
ν_{18}	b$_2$	786(5)	780
ν_{12}	b$_1$	512(6)	511
ν_{11}	b$_1$	740(6)	756
ν_9	a$_2$	545(6)	560
ν_8	a$_2$	852(6)	874
ν_7	a$_1$	898(6)	919
ν_6	a$_1$	969(6)	982
ν_5	a$_1$	1139(6)	1166
ν_4	a$_1$	1284(6)	1313
ν_3	a$_1$	1378(6)	1436

[a]The numbers in the parentheses indicate the experimental uncertainties in the last digit.
[b]The theoretical frequencies are calculated at the B3LYP/6-311++G** level of theory (see Table S7). These data are the same as those reported in ref. 10 computed at the same level of theory.

Table S4. The theoretical frequencies of pyrrolyl.

Symmetry	Mode	ω (cm^{-1})[a]	ω (cm^{-1})[b]
a1	ν_1	3246	3275.1
	ν_2	3201	3230.7
	ν_3	1556	1549.1
	ν_4	1433	1447.3
	ν_5	1202	1188.6
	ν_6	1090	1084.2
	ν_7	1043	1039.1
	ν_8	882	869.5
a2	ν_9	904	885.3
	ν_{10}	817	815.0
	ν_{11}	488	488.7
b1	ν_{12}	835	815.6
	ν_{13}	710	700.9
	ν_{14}	540	541.0
b2	ν_{15}	3227	3254.2
	ν_{16}	3197	3226.2
	ν_{17}	1355	1349.0
	ν_{18}	1293	1284.3
	ν_{19}	1079	1069.4
	ν_{20}	935	924.6
	ν_{21}	664	668.3

[a]The theoretical frequencies are calculated at the B3LYP/6-311++G** level of theory.

[b]The harmonic frequencies are from reference 9, calculated at the fc-CCSD(T)/ANO level of theory.

Table S5. The theoretical frequencies of imidazolyl.

Symmetry	Mode	ω (cm^{-1})^a
a1	ν_1	3231
	ν_2	3218
	ν_3	1436
	ν_4	1313
	ν_5	1166
	ν_6	982
	ν_7	919
a2	ν_8	874
	ν_9	560
b1	ν_{10}	867
	ν_{11}	756
	ν_{12}	511
b2	ν_{13}	3205
	ν_{14}	1523
	ν_{15}	1289
	ν_{16}	1188
	ν_{17}	1016
	ν_{18}	780

^{a}The theoretical frequencies are calculated at the B3LYP/6-311++G** level of theory. These data are the same as those reported in ref. 10 computed at the same level of theory.

Table S6. The theoretical frequencies of 2-pyrrolyl.

Symmetry	Mode	ω (cm^{-1})^a	ω (cm^{-1})^b
a'	ν_1	3675	3695.4
	ν_2	3263	3295.3
	ν_3	3258	3286.9
	ν_4	3228	3259.1
	ν_5	1549	1562.9
	ν_6	1453	1460.8
	ν_7	1403	1412.6
	ν_8	1359	1373.8
	ν_9	1252	1245.7
	ν_{10}	1170	1166.8
	ν_{11}	1103	1103.8
	ν_{12}	1057	1060.2
	ν_{13}	1022	1020.7
	ν_{14}	888	878.9
	ν_{15}	855	846.0
a''	ν_{16}	856	842.0
	ν_{17}	753	750.0
	ν_{18}	683	695.7
	ν_{19}	616	610.6
	ν_{20}	455	499.3
	ν_{21}	292	325.8

^{a}The theoretical frequencies are calculated at the B3LYP/6-311++G** level of theory.
^{b}The harmonic frequencies are from reference 9, calculated at the fc-CCSD(T)/ANO level of theory.

References

1   L. S. Wang, *J. Chem. Phys.*, 2015, **143**, 040901.
2   L. S. Wang, C. F. Ding, X. B. Wang and S. E. Barlow, *Rev. Sci. Instrum.*, 1999, **70**, 1957–1966.
3   X. B. Wang and L. S. Wang, *Rev. Sci. Instrum.*, 2008, **79**, 073108.
4   I. León, Z. Yang, H. T. Liu and L. S. Wang, *Rev. Sci. Instrum.*, 2014, **85**, 083106.
5   G. A. Garcia, L. Nahon and I. Powis, *Rev. Sci. Instrum.,* 2004, **75**, 4989–4996.
6   V. Dribinski, A. Ossadtchi, V. A. Mandelshtam and H. Reisler, *Rev. Sci. Instrum.*, 2002, **73**, 2634–2642.
7   M. J. Frisch, G. W. Trucks, H. B. Schlegel, G. E. Scuseria, M. A. Robb, J. R. Cheeseman, G. Scalmani, V. Barone, G. A. Petersson, H. Nakatsuji, X. Li, M. Caricato, A. Marenich, J. Bloino, B. G. Janesko, R. Gomperts, B. Mennucci, H. P. Hratchian, J. V. Ortiz, A. F. Izmaylov, J. L. Sonnenberg, D. Williams-Young, F. Ding, F. Lipparini, F. Egidi, J. Goings, B. Peng, A. Petrone, T. Henderson, D. Ranasinghe, V. G. Zakrzewski, J. Gao, N. Rega, G. Zheng, W. Liang, M. Hada, M. Ehara, K. Toyota, R. Fukuda, J. Hasegawa, M. Ishida, T. Nakajima, Y. Honda, O. Kitao, H. Nakai, T. Vreven, K. Throssell, J. A. Jr. Montgomery, J. E. Peralta, F. Ogliaro, M. Bearpark, J. J. Heyd, E. Brothers, K. N. Kudin, V. N. Staroverov, T. Keith, R. Kobayashi, J. Normand, K. Raghavachari, A. Rendell, J. C. Burant, S. S. Iyengar, J. Tomasi, M. Cossi, J. M. Millam, M. Klene, C. Adamo, R. Cammi, J. W. Ochterski, R. L. Martin, K. Morokuma, O. Farkas, J. B. Foresman and D. J. Fox, Gaussian 09, Revision D.01, Gaussian, Inc., Wallingford CT, 2016.
8   I. Pugliesi and K. Müller-Dethlefs, *J. Phys. Chem. A*, 2006, **110**, 4657–4667.
9   S. L. Johansen, Z. Xu, J. H. Westerfield, A. C. Wannenmacher and K. N. Crabtree, *J. Phys. Chem. A*, 2021, **125**, 1257–1268.
10   A. J. Gianola, T. Ichino, R. L. Hoenigman, S. Kato, V. M. Bierbaum and W. C. Lineberger, *J. Phys. Chem. A*, 2005, **109**, 11504–11514.